

**Effects of nearby ordered domains, target receptors
and phospholipid bilayers on conformations of an
intrinsically disordered protein**

DOCTORAL DISSERTATION PROPOSAL

BY

RUCHI LOHIA



**CENTER FOR COMPUTATIONAL AND INTEGRATIVE
BIOLOGY**

RUTGERS UNIVERSITY

CAMDEN, NJ-08012

May 2014

1 Objectives

Intrinsically Disordered Proteins (IDPs), are proteins that are functional without having a unique folded 3 dimensional (3D) structure. They are highly abundant, involved in critical biological functions and are associated with various diseases. However, because of heterogeneous nature of IDPs, characterizing all its conformations using standard experimental techniques is challenging. Molecular simulation therefore can play an important role in understanding their dynamics.

Precursor brain-derived neurotrophic factor (proBDNF) is an example of a hybrid protein having a disordered prodomain and an ordered mature domain (mBDNF). It is essential for neuronal survival and regulation of synaptic plasticity. A common Val66Met substitution in its disordered prodomain is strongly associated with various neuropsychiatric disorders, but the mechanism of its action is unknown.

With our proposed research we aim to study the dynamics of a disordered prodomain on the presence of its ordered domain and/or target receptor, a phospholipid bilayer, as well as the effects of a common single nucleotide polymorphism (SNP) on its behavior. Altogether the proposed study will help in understanding the structural and conformational properties of BDNF and its interactions with other proteins. In addition it will also contribute to better understanding of IDPs in general.

Aims:

- 1) Characterizing the conformational ensemble of wild type proBDNF and Val66Met mutant.** At present the effects of Val66Met substitution on the dynamics of the disordered prodomain and the interactions of the prodomain with the mBDNF

in proBDNF structure is not known. We will use Molecular dynamics (MD) simulations with enhanced sampling method (**Section 5: General Procedures**) to characterize the conformational ensemble of prodomain and proBDNF with and without the SNP.

2) Characterizing the conformational ensemble of proBDNF in complex with its receptor p75^{NTR}. To investigate the dynamics and interactions of prodomain in proBDNF:p75^{NTR} receptor complex and to rationalize how prodomain mediates receptor specificity, conformational ensemble of proBDNF bound to its receptor p75^{NTR} will be generated. We will use MD simulations with enhanced sampling method (**Section 5: General Procedures**) to characterize the ensemble.

3) Characterizing the conformational ensemble of juxtamembrane domain of p75^{NTR}. At present it not known how the presence of a phospholipid bilayer affects the disordered conformational ensemble. To address the above questions the conformational ensemble of disordered juxtamembrane domain of p75^{NTR} will be generated using MD with enhanced sampling technique (**Section 5: General Procedures**).

2 Background

2.1 Disordered Proteins

Disordered regions show low sequence conservation[1] and are associated with high frequency of SNPs[2]. It has been shown that 21.7 % of missense disease mutations are found in disordered regions.[3].

Previously, functional proteins were viewed as having a unique folded conformation

under physiological conditions, characterized by their relatively fixed atom positions and backbone dihedral angles. Generally, these proteins fit the structure-function paradigm, in which the function of protein is determined by its unique 3D structure[4]. In the last 10 years many proteins and protein regions have been shown to be intrinsically disordered in their functional form[5, 6]. Challenging the structure-function paradigm these proteins lack a unique 3D structure and exist as wide ranging conformational ensembles, from completely unstructured random coils to compact molten globules with local elements of secondary structure[7]. However, according to predictions from polymer physics the IDPs typically possess the expected behavior of flexible and charged polymers[8, 9].

It suggests that water at ambient temperature is a poor solvent for polypeptide backbone, which make IDPs in general compact, with electrostatic interactions having a basic influence on the final state[9]. More than 75% of the IDPs are polyampholytes[10]. The fraction of charged residues(FCR) discriminates between weak and strong polyampholytes. Weak polyampholytes shows conformational preference for compact globules whereas, conformational preference for strong polyampholytes ($FCR > 0.35$) further depends on its linear sequence distributions of oppositely charged residues. For well mixed charged distributions electrostatic repulsions and attractions are counterbalanced, leading to conformational preference that resembles self-avoiding random walks (excluded volume limit) or generic Flory random coils(FRC). Segregation of oppositely charged residues form hair-pin like conformations caused by long range electrostatic attractions. Most of the IDPs have well mixed charges, thus, it shows a preference for random coil conformers[9].

The intrinsic disorder can be linked to the primary amino acid sequence, generally

characterized with high charge density, low hydropathy[11], low sequence complexity[12], low inter residue interactions energies[13]. They also show significant depletion of order promoting amino acids (Trp, Tyr, Phe, Ile, Leu, Val, Cys, and Asn)[14]. With the increasing attention to IDP's, more than 30 disorder predictor are currently available[15].

IDPs have been shown to be abundant in all kingdoms of life for example 33 % of eukaryotic proteins have long (>30 residues) disordered regions (IDRs) [16]. Seventy percent of protein structures deposited in PDB have portions of their sequence of missing electron density[17]. IDPs and IDRs play key roles in transcription regulation, cell signaling and control pathways[18]. They mediate post-translational modification (phosphorylation) and function as hubs in protein-protein interaction network.[19].

High conformational flexibility of these proteins gives them several advantages like increased interaction area per residue('fly-casting')[20], ability to bind multiple partners[18] and ability to bind with high specificity and low affinity. These proteins might act as linkers for two globular domains[21], tails that modulate the function of structured domain , undergo coupled folding and binding in the presence of a ligand/receptor[22, 23] or remain disordered even in the bound state (Fuzzy complexes)[24, 25].

Understanding the dynamics and functional mechanisms of IDPs is a very active research field.Conformational selection (IDP in the absence of the binding partner is biased towards the bound conformation) [26, 23], ‘induced fit’ (the binding partner induces the IDP to adopt bound conformation) or combinations of these models have been proposed in coupled folding and binding of IDPs[22]. The role of preformed structural elements in IDP's is controversial. These elements in unbound ensemble of IDPs have been shown to be critical in some binding reactions[27, 28, 23] and unessential for others[29].

The abundance, biological importance and association with diseases makes IDPs an exciting target for protein research and drug discovery. Unlike ordered proteins, IDPs sample multiple conformations while retaining some residual structure. Experimental techniques generally provide only ensemble averaged properties thus, characterizing all the conformations belonging to an ensemble of IDP is challenging[30]. Molecular simulations are a powerful technique for such characterization and have been shown to play an important role in understanding their behavior[26, 31].

2.2 Brain-derived neurotrophic factor

The family of Neurotrophins (NT) are proteins secreted in the nervous system that aid in neuronal circuit development including neuronal survival, process outgrowth and regulation of synaptic plasticity (for reviews [32, 33]). Four members belonging to the family of NT have been discovered; nerve growth factor(NGF)[34, 35], brain derived neurotrophic factor(BDNF)[36], neurotrophin-3(NT-3)[37], neurotrophin-4(NT-4)[38]. NTs have a similar range of functions, but are directed against different cell populations.

NTs are initially synthesized as propeptides(240-260)(pro-neurotrophins) and are proteolytically cleaved to form an N-terminal prodomain and a C-terminal mature domains(-120)[39](Figure 1). After translation propeptide (pro-neurotrophin) associate as noncovalent homodimers via interactions of the mature domain[40, 41]. All the mature neurotrophins are evolutionary conserved and structurally related with the sequence identities approaching 50%[42] and the prodomains have few segments of sequence identity[39]. BDNF and NGF prodomains have been shown to be intrinsically disordered[43, 44].

The present study focuses on BDNF; It is the best-studied neurotrophic protein that

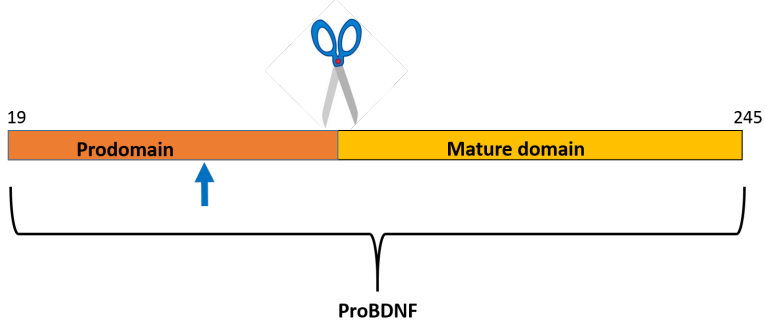


Figure 1: A schematic representation of proBDNF and the proteolytic cleavage site. The arrows indicates the location of Val66Met substitution.

plays major role in regulating neuronal activity-dependent plasticity in the brain, including hippocampal long term potentiation (LTP)[32, 45]. Additionally, a Val66Met substitution in its disordered prodomain has been associated with various neurophysiologic disorders such as Alzheimer’s disease [46]. proBDNF can undergo intracellular or extracellular proteolysis to generate mBDNF[47, 48]. Both mBDNF and proBDNF can be secreted from neurons in an activity dependent manner and can mediate contrasting functions via different class of receptors[49, 44]. Figure 2 summarizes the BDNF functional forms and its receptors.

Mature domain structure and function: High resolution structures have been determined for each of the mature neurotrophins[50, 51, 52]. They exist as non-covalent homodimers[41]. Each protomer shares a common fold comprising 8 beta strands and is locked by an interchain cysteine knot. The loop regions with low sequence similarity shows structural variations and are assumed to be flexible in vivo[52].

Mature NT binds to one of the tropomyosin-receptor-kinase (Trk) class of receptors (TrkA, TrkB, TrkC) to promote neuronal survival and development via receptor dimerization, where the specificity is mediated by the disorder to order transition of N-terminal

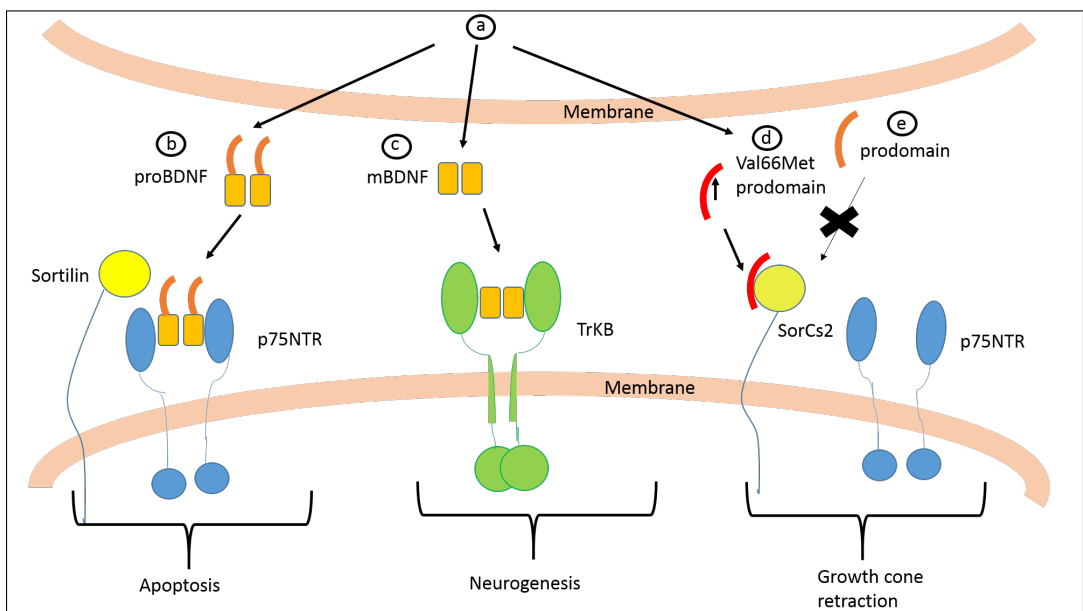


Figure 2: Schematic representation of mature BDNF, proBDNF and prodomain actions as well as the diversity of coreceptor interactions in the central nervous system.(a) proBDNF, mBDNF, prodomain and Val66Met prodomain can be secreted from neurons in an activity dependent manner. (b) proBDNF forms ternary complex with Sortilin and p75^{NTR} which initiates nerve cell death. (c) mBDNF binds TrkB and thereby promotes neuronal survival (d) Val66Met prodomain binds SorCs2 in p75^{NTR} positive cells which induces growth cone retraction (e) Binding of native prodomain with SorCs2 in p75^{NTR} positive cells does not induce growth cone retraction.

residues (5-12) of mature domain, as observed in the crystal structures of NGF, NT4/5 in complex with TrkA and TrkB respectively[53, 54].

proBDNF structure and function: No studies regarding whole proBDNF structure determination have been reported. Few studies done to characterize structure of homologue proNGF have determined it to be flexible, with a possible intramolecular interaction of the NGF prodomain with the mature region[43, 55]. Crystallographic analysis of the proNGF has been hindered because of its intrinsic flexibility and susceptibility to cleavage, hence crystal structure of proNGF bound with receptor p75^{NTR} is available but the density of prodomain is missing[56].

Most growth factors are synthesized as precursors, and prodomains have been demonstrated to play a critical role in ensuring proper protein folding[39] and intracellular sorting[57]. In the past 10 years, studies suggested that pro-neurotrophins serve as signaling molecules rather than inactive precursors [58]. Pro-neurotrophins do not activate Trk receptor, in contrast, pro-neurotrophins bind p75^{NTR} (tumour necrosis factor superfamily receptor) with high affinity [59, 60]. proBDNF can interact with diverse receptors
1) Interaction of proBDNF and p75^{NTR} is associated with Long Term Depression[61].
2) A co-receptor Sortilin (a Vps10p-domain sorting receptor family member) specifically recognizes the prodomain and forms a high affinity ternary complex with proBDNF and p75^{NTR} leading to nerve cell death [62]
3) proBDNF and p75^{NTR} induces growth cone retraction in the presence of SorCS2 (sortilin-related VPS10 domaincontaining receptor [63, 64, 44].

p75^{NTR} structure and functional mechanism: p75^{NTR} is the first neurotrophin receptor to be identified[65]however, now it is one of the 25 members of TNF receptor superfamily of receptors, which is structurally characterized by having extracellular cysteine-rich domains (CRDs) and an intracellular death domain[66](Figure 3). Apart from binding NTs it can act as a coreceptor for diverse ligands that exhibit distinct biological activities. It can trigger various responses including axonal retraction, apoptosis, and modulation of synaptic plasticity on NT binding[33].

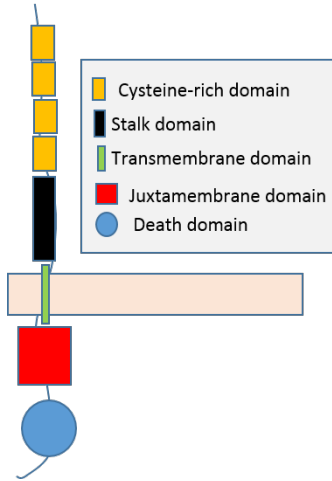


Figure 3: The CRDs (~ 190 residues) are attached to an extracellular stalk that is involved in the sorting of p75^{NTR} (~ 60 residues). The transmembrane domain is a single helix highly conserved across species (~ 21 residues). The intracellular region contains the juxtamembrane domain (~ 80 residues) followed by the carboxy-terminal domain, which contain a globular, six-helix death domain (~ 90 residues)[66].

p75^{NTR} is a non-catalytic receptor, thus, unlike ligand-mediated dimerization mechanism, it is thought to proceed via ligand-dependent recruitment and release of cytoplasmic effectors to and from the receptor. Large number of intracellular interactors of p75^{NTR} have been identified but its activation mechanism remains elusive[33, 67]. Crystal structures of p75^{NTR} with proNGF and NT-3 reveals 2:2 stoichiometry binding[68, 56]. p75^{NTR} exists as dimer in vitro mediated via non-covalent interactions of a conserved motif (AxxxG266) in its transmembrane domain[67]. Conformational changes in the intracellular

lular domain of disulfide-linked (CYS257) p75^{NTR} dimer appears to be a trigger on NT binding[67, 56]. However, how does p75^{NTR} can execute downstream signaling events unique to a given proneurotrophin is unknown.

The polypeptide segment connecting the transmembrane and death domains (Juxtamembrane) has been shown to be highly flexible[69]. This juxtamembrane linker might be playing critical role in propagation of the conformational differences to the death domain induced by binding of various ligands to the extracellular domain.

BDNF prodomain and Val66Met polymorphism: Recent reports have documented that the prodomain of BDNF is detectable *in vivo* [70, 44]. It have been found in monomeric state and is characterized as intrinsically disordered. A common SNP in the BDNF gene leads to Val66Met substitution in its prodomain. More than 25% of human population is heterozygous(SNP Database, NCBI, 2012) and 4% population is homozygous for this SNP[71]. It is associated with various effects including 1) poor episodic memory [72] 2) reduction in hippocampi volume[46] 3) enhanced risk of anxiety disorders such as bipolar disorder and Parkinson's and Alzheimer's diseases [46, 73] 4) unresponsiveness to antidepressant, fluoxetine[74, 75]. These effects have been attributed to 1) altered intracellular trafficking of BDNF mRNA [76] 2) decreased targeting of Val66Met to secretory granules mediated via decreased binding to intracellular sorting protein Sortilin[57], altogether leading to selective impairment in the activity- dependent release of BDNF [77, 57]. Additionally, recently it was shown that isolated Met66 (and not Val66) prodomain can bind deferentially to SorCS2 and promotes growth cone retraction in the cells co-expressing p75^{NTR}[44].

3 Preliminary Studies

As discussed in the **Section 2: Background**, a common SNP in the BDNF prodomain confers bioactivity[44]. An essential step to investigate the distinct biological functions of prodomain versus Val66Met prodomain and to rationalize how the M66 prodomain confers bioactivity would be establishing the prodomain structure. However, the prodomain is disordered and thus, does not have one stable conformation. Experimental studies of BDNF prodomain could not study the entire prodomain or address its dynamics. Molecular simulations can therefore play an important role in the understanding of prodomain behavior, as they provide a detailed picture of the dynamics in unfolded proteins[31]. No molecular dynamics simulation of BDNF prodomain has been reported so far.

Force field selection: MD simulations offer the potential to gain new insight into the dynamics and functional mechanisms of biomolecules. However, all atom simulations of proteins faces two major limitations: 1) The computational demanding nature of molecular simulations restricts the simulation time thus, prevents a simulation from reaching biologically relevant time scales. Several enhanced sampling techniques have been developed which allows to efficiently explore the configurational space in relatively shorter simulation time[78] (discussed in more detail in **Section 5: General Procedures**). Additionally, advances in both software and hardware have made possible the simulation on timescales well beyond the microsecond[79]. 2) Inaccuracies of the empirical force field (FF) may produce misleading results. There are several FF available and their quality have been continuously improving, however, every force field has several limitations and may not be completely transferable for e.g C22/CMAP is biased towards α -helical conformations[80].

Force fields may be tested by their ability to reproduce and predict experimental observables[80, 81]. We used this procedure for choosing suitable force field for our system. A recent nuclear magnetic resonance (NMR) study for the BDNF prodomain and Val66Met BDNF prodomain reported that the M66 prodomain (M form) has more helical propensity for the residues around the SNP (55-76) as compared to V66 prodomain (V form). We did 10 different 60ns long simulations of the residues 55-76 for both M form and V form using two different force field (CHARMM36[80] and AMBER99SB[81]). Figure 4 shows the ensemble averaged time spent by each residue in α -helix conformation. AMBER99SB force field shows more reasonable agreement with NMR predictions. Further simulations have used a more recent version of AMBER99SB FF; AMBER99SB-IDLN[82].

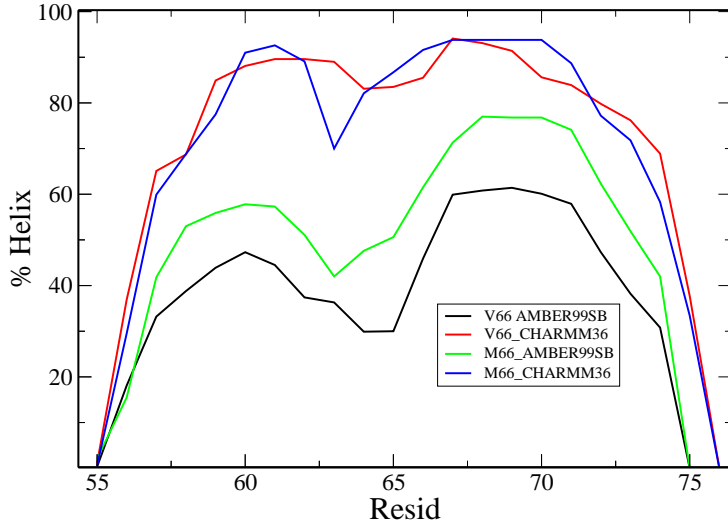


Figure 4: Helix propensity for residues 55-76 of prodomain with two different force field. Using AMBER99SB force field M form shows more helical propensity (green) when compared to V form (black), this is in agreement with the NMR studies. Using CHARMM36 force field M form (blue) and V form (red) shows high and equal propensity of helix formation. NMR studies suggest low to moderate degrees of helical structure in prodomain at residue 66, also more consistent with the AMBER99SB forcefield.

Simulation of native prodomain and Val66Met prodomain: The prodomain spans from residue 19 -128 (109 residues). Apart from NMR studies various disorder predictors such as Foldindex[83], Globplot[84], Iupred[13] predicts the prodomain to be disordered. We conducted molecular simulation of both V form and M form from region 24-128 (105 residues) using enhanced sampling temperature replica exchange method (T-REMD) to overcome the sampling problem. Most previous studies using REMD have been conducted for smaller IDPs (40-70 residues long)[31].

Simulation setup: The prodomain model previously constructed was heated to generate a random coil configuration. The M form was generated by mutating Val 66 to Met using mutator plugin in VMD. The system was setup using GROMACS 4.6.3 package with AMBER99SB-IDLN force field for both M and V form. Dodecahedron waterbox with padding 1.1 Å, salt concentration 0.15M (NaCl) and TIP3P water model was used. The system size was approximately 76,000 atoms. It was simulated at 300K and constant pressure for 7ns. From the resulting trajectory, a conformation with volume close to the average volume of the trajectories was selected. To produce different starting random coil conformation for each replica, the selected structure was simulated at constant volume at high temperature (600K) for 10ns. Conformations with more than 30ps interval and correct proline conformations (since proline may isomerise at higher temperature) were selected. Each conformation was then equilibrated at its appropriate starting temperature for 5ns.

After this preparation T-REMD simulations were done for both M and V form with 60 replicas in the temperature range of 300 K to 420 K. Each replica was simulated for 260ns, giving a total simulation time of $30\mu\text{s}$. The average exchange acceptance

probability was 0.17 (range 0.102 - 0.242) for V form and 0.21 (range 0.07-0.38) for M form, with exchange frequency of 1ps. After discarding the first 50ns as equilibration run, replicas at the lowest temperatures (300 K) were analyzed. The structures with root mean square deviation(rmsd) < 1.5 Å after fitting were grouped together as one cluster. Figure 5 depicts the conformations of the three most populated clusters for both V and M form. The most populated cluster represented < 5 % of the total frames and top 10 most populated clusters represented <21 % of total frames. Thus, none of the clusters were most dominating. It reiterates the observation that the prodomain is intrinsically disordered.

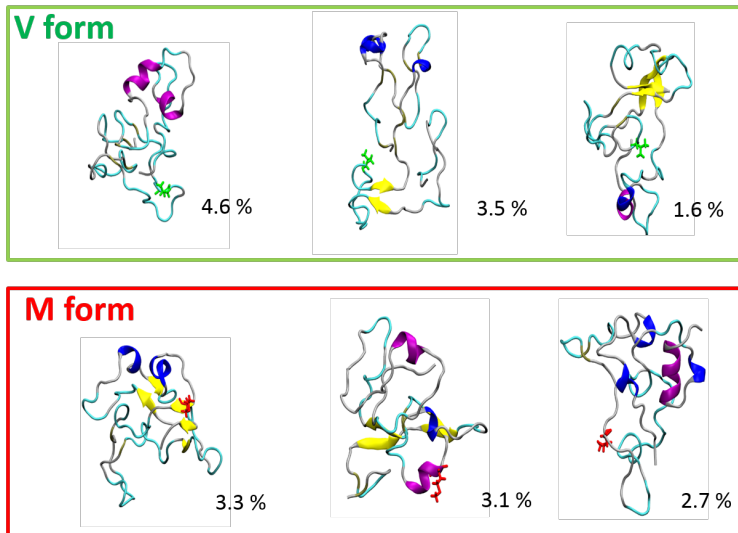


Figure 5: A representative structure is drawn from each of the three most populated clusters for both V form (top panel) and M form (bottom panel). The number on the right of each conformation denotes the percentage of frames in that cluster. The trajectories were generated using VMD.

3.1 Preliminary Results and Discussion

The structural ensembles of IDPs have many features, local and global which are critical for the functioning of the protein. Local features include the presence of prestructured

motif which can be critical for binding. Global hydrodynamic features might be important in regulating accessibility/exposure of motifs and also for long range communications between different parts of the protein.

Residual Secondary Structure: IDPs lack stable secondary or tertiary structure under physiological conditions although, they can have transient secondary structures. The NMR studies of prodomain, found it to be intrinsically disordered with some differential residual secondary structure preferences for M form and V form. In order to compare the secondary structure propensity of our simulated prodomain with experimental observations, we analyzed the helical tendency in the 300 K replica. Figure 6 shows the time spent by each residue in the helical state. In our simulations we observe increased helical tendency in the region 63-66 in accordance with the NMR studies. Apart from residues around the SNP, we also observe some secondary structure change at residue (resid) 70-75, 90-95 and 103-105. How the mutation can plausibly cause these distant secondary structure changes can be investigated by accessing the changes in its global conformation.

Dihedral angles free energy surface: To have a closer look at residue 66 dynamics, we calculated Gibbs free energy landscapes for its dihedral ϕ and ψ angles for both V and M form. This free energy surface (Figure 7) reveals that for V form at resid 66, there are two wells, one in the α helix region and one in the β sheet region but M form has an additional well at left-handed α helix. Additionally, the well at β sheet region is deeper and has a higher barrier between α helix and β sheet region for V form compared to M form. The above observations suggest that although both V and M form has minima

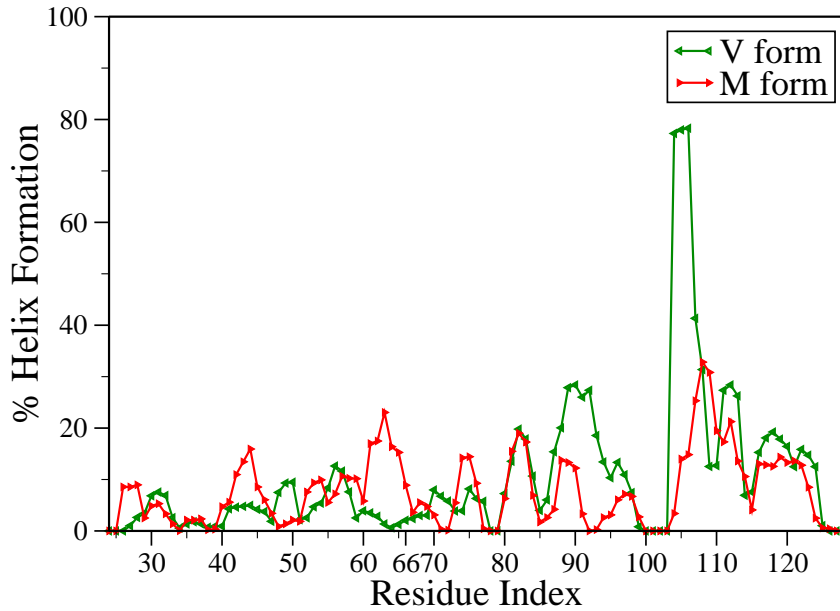


Figure 6: Red and green curves shows the probability of forming α helix in M and V form respectively. The residues 60-65, 70-75 and 90-95 shows differential probability of helix formation. The assignment of secondary structure was done using STRIDE in VMD.

around the α helix region, V form has a deeper minima for beta sheet region with a higher barrier, this may allow some of the Val 66 to get trapped in the β region.

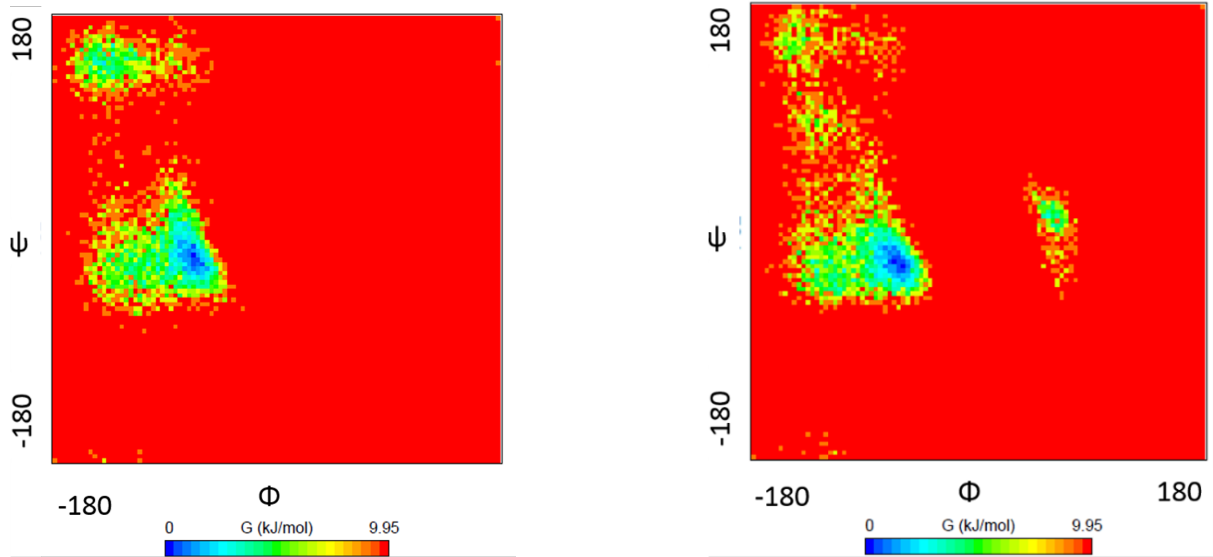


Figure 7: Gibbs free energy landscape of ϕ and ψ angles at residue 66 for the conformational ensembles of V form (left) and M form (right). With the increase in free energy the color transits from cooler to hotter. V form forms a deeper well in β sheet region and also has high barrier between the β sheet and α helix region. This can be related to its lower probability of forming α helix.

SNP effects the globular structure of the protein: In addition to individual residues, we can look at larger sections of the prodomain, and compute its conformational properties, in order to evaluate the effects of mutation on its dynamics and behavior. The left panel of Figure 8 shows the distribution of conformations of both M and V form on the first two components, calculated using dihedral principal component analysis(dPCA). M and V form forms separate clusters on the first principal component (PC1), residues around the SNP mediates 18.5 % of this total conformational fluctuation, although, few residues distant from the SNP also causes significant impact on conformation fluctuation.

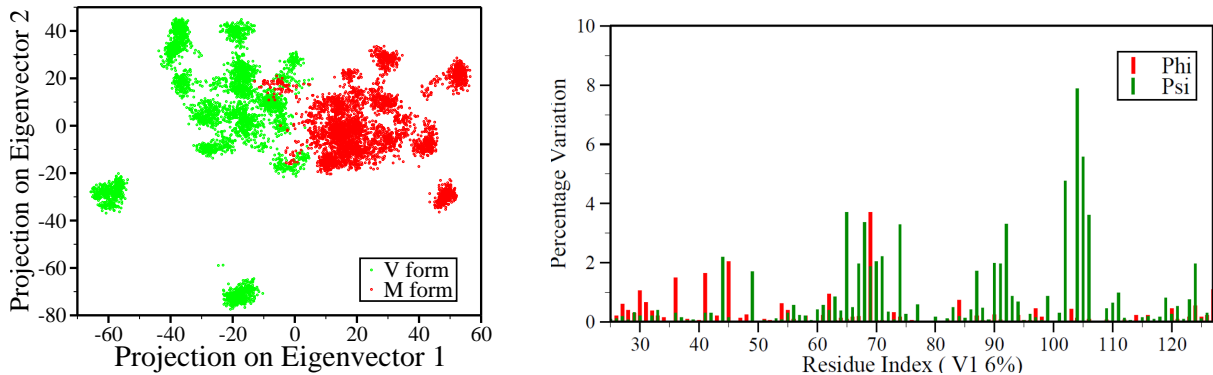


Figure 8: (Left) After performing dPCA, the distribution of conformations of V form (green) and M form (red) on the first two principal components. (Right) Influence of each residue dihedral angles ϕ (red) and ψ (green) on the first principal component. The first principal component contributes 6% to the overall fluctuation of the system.

Figure 9 shows the contact maps for V and M form. It reveals that M form shows higher dispersion and forms differential contacts with the end regions. Figure 10 shows that residues around the SNP, region III and region V, interacts more strongly with the N- and C-terminal regions in V form. The N- and C-terminal is mostly interacting with itself in M form (region I and IV). Root mean square fluctuation (RMSF) is a traditional way of measuring protein backbone flexibility. The right panel of Figure 9 compares the RMSFs for M and V form. It shows that M form is comparatively more flexible

throughout its amino acid sequence.

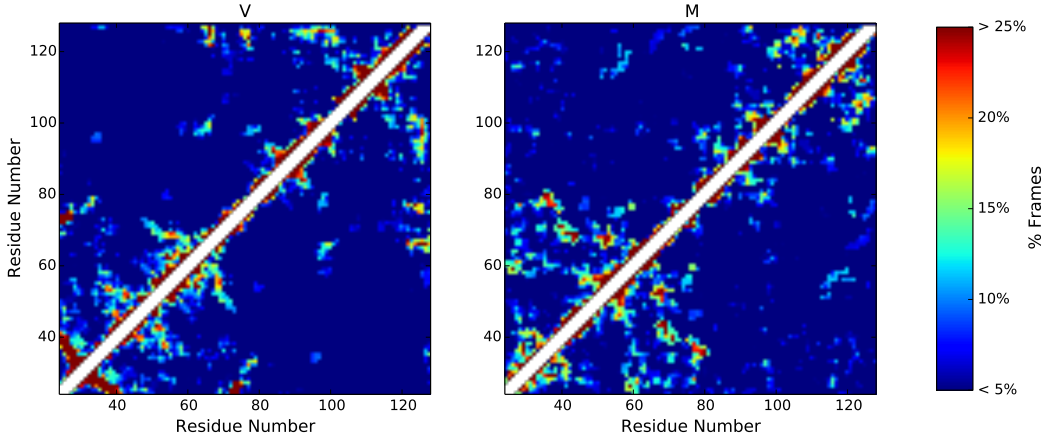


Figure 9: Contact map for V form (left) and M form (right). As the probability of contact formation increases the color transits from cooler to hotter ones. M form shows higher dispersion. A pair of residues is considered to be in contact if any pair of non-hydrogen atoms from two residues are within 4.5\AA of one another.

Valine is considered inherently more hydrophobic than Methionine[85]. The extent to which residues are buried in a protein conformation depends not only upon strict hydrophobicity but also upon steric effects that determine packing between the crowded interior of the protein[85]. Nevertheless, we observe that fewer hydrophobic interactions in M form can be a plausible explanation for its higher flexibility and differential contacts formation with the N- and C-terminal, although sampling limitations can always be a possible reason.

Solvent Accessible Surface Area(SASA): Experimental studies with the prodomain identified M form as a new active ligand which can bind differentially, at residues around the SNP (65-71) with SorCS2 and induce growth cone retraction. In our simulations we observe high solvent accessible surface area around this region which can be associated with stronger binding in this region (Figure 11).

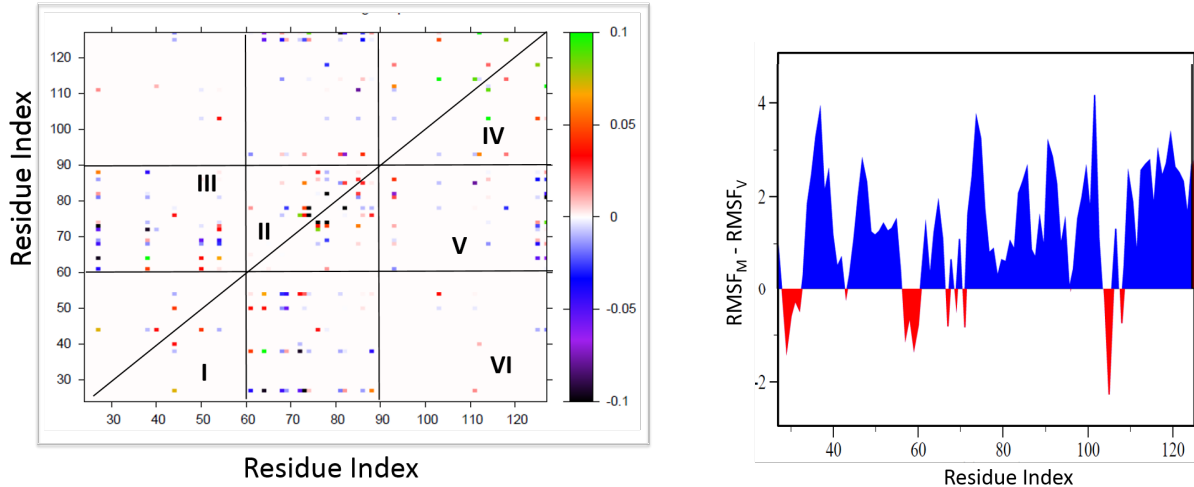


Figure 10: (Left) Differential probability of salt bridge formation. As the probability increases in V form the color transits from hotter to cooler one. Regions around the SNP shows higher salt bridge formation with the end terminals in V form (II and V). The C and N-terminal regions are interacting within themselves in M form (I and V). (Right) Difference RMSF plot for M and V form. Regions above the x axis (blue) indicates higher flexibility in M form and regions below the x axis (red) indicates higher flexibility in V form.

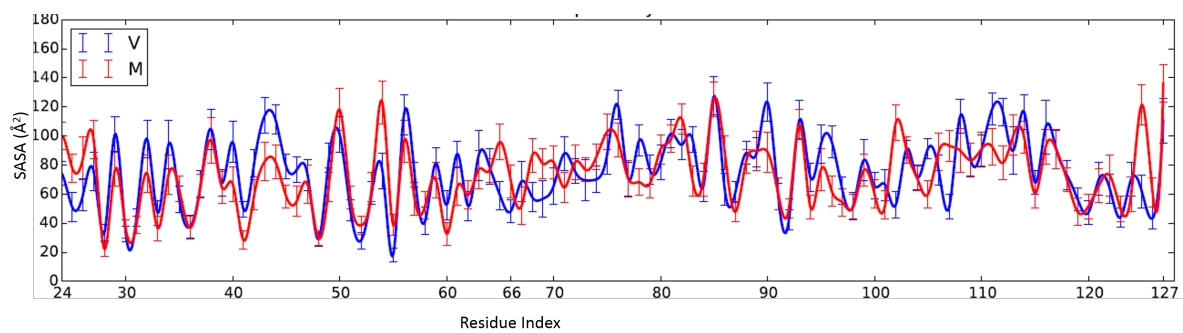


Figure 11: M form (red) shows increase in solvent accessible surface area at differential binding site (residues 65-71) when compared with V form (blue). Solvent accessible surface area was calculated using Gromacs tool with solvent probe radius of 1.4 Å.

Comparison with experimental data: To assess how close our computed ensemble is to that observed experimentally, we back-calculated chemical shifts from our simulations results using SPARTA+, and compared them with the experimental values. Random coil shifts from the primary amino acid sequence were also calculated[86] and compared. The simulation correctly reproduces the locations and extensions of the helices, as Figure 12 but, these also very close to the random coil shifts. This also suggests that the prodomain doesn't form very stable secondary structures and is mostly disordered.

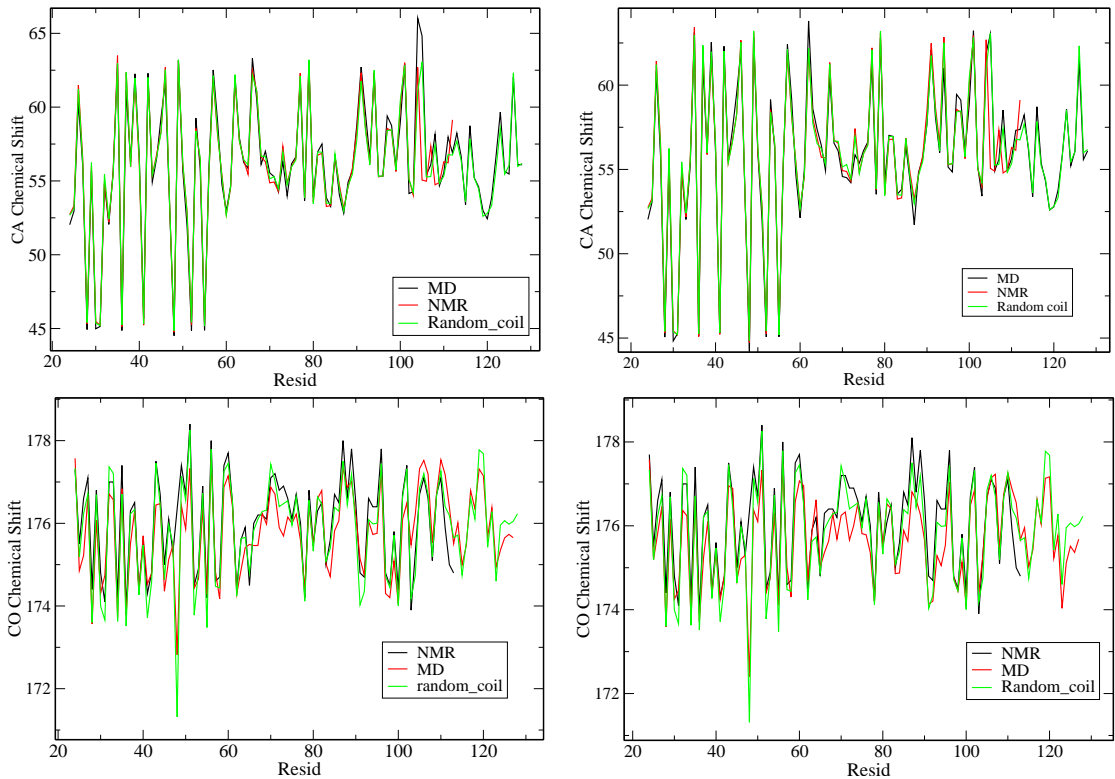


Figure 12: Chemical shifts calculated with SPARTA+ from the simulations (black) and random coil index calculated from primary amino sequence (green) are compared with the experimental values (red). Right panels are for V form and left panels are for M form.

Radius of Gyration (R_G): R_G of a molecule gives us the measure its compactness. M form shows more number of multiple peaks for rgyr distribution Figure 13. Using the relation between R_G and hydrodynamic radius (R_H) ($R_H \sim 0.75 * R_h$) we calculated the

R_H from our simulation. The calculated R_H ; $\sim 20 \text{ \AA}$ for V form and $\sim 19.7 \text{ \AA}$ for M form, is comparable to the experimentally measured R_H of $22.4 \text{ \AA} \pm 0.05$ and $22 \text{ \AA} \pm 0.05$ respectively.

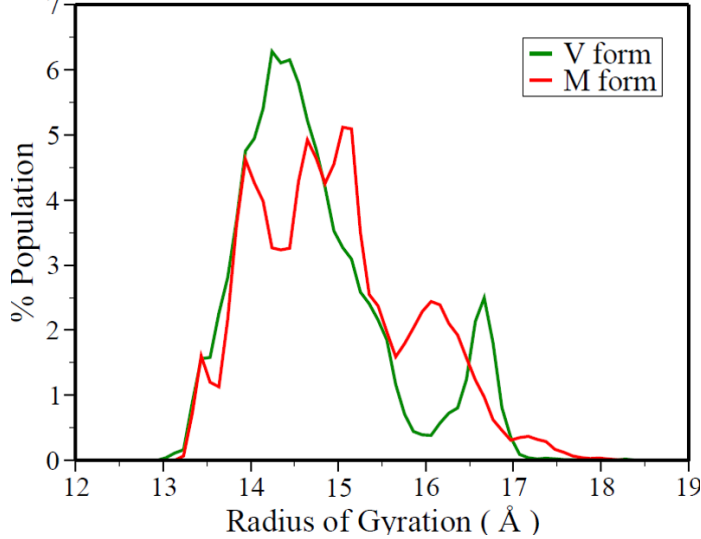


Figure 13: Radius of gyration distribution of V form (green) and M form (red). M form shows more number of multiple peaks in the distribution.

Polymeric properties of disordered prodomain: Polymer theories offers a much improved insight into the sequence ensemble relationships of polyampholytic IDPs. BDNF prodomain is a polyampholyte with 0.106 f+ and 0.154 f-, where f+ and f- denotes the fraction of positive and negative charged residues. The fraction of charged residues (FCR) is 0.259 and net charge per residue (NCPR) is 0.048. This combination of FCR and NCPR places it on the boundary of weak and strong polyampholyte like many other IDPs[9] and it will likely show conformational preference for Flory Random Coil (FRC) (extended molten globules) or compact molten globule.

Right panel of Figure 14 plots the ensemble-averaged inter-residue distances against sequence separations $|j-i|$. Both Val form and M form shows conformational preference for compact molten globule with slight differences in the packing. Left panel of Figure 14 eval-

uates the globule packing with respect to residue 66. It shows that Val form forms closer contacts with the C-terminal region (mostly basic and hydrophobic residues). Figure 15 shows that increasing temperature causes weak contraction / expansion in different regions. The ensembles does not show pronounced temperature dependence.

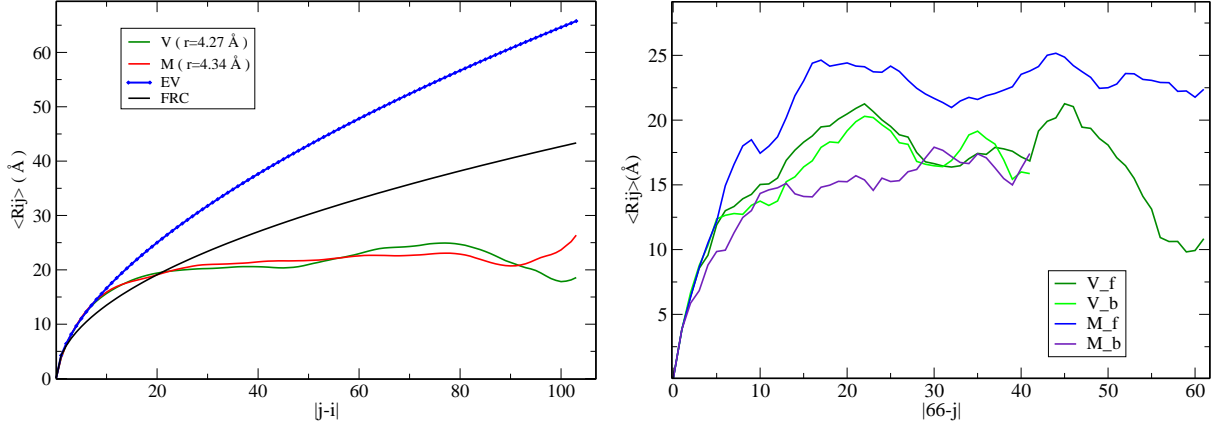


Figure 14: (Right) $\langle R_{ij} \rangle$ profiles for V form (green) and M form (red). The blue curve denotes the profile expected for the prodomain in the EV limit. The black curve is expected profile for an FRC[9]. r denotes the persistence length. (Left) $\langle R_{ij} \rangle$ profile at residue 66. f and b denotes all the residues which are ahead and before residue 66, respectively in the prodomain primary sequence.

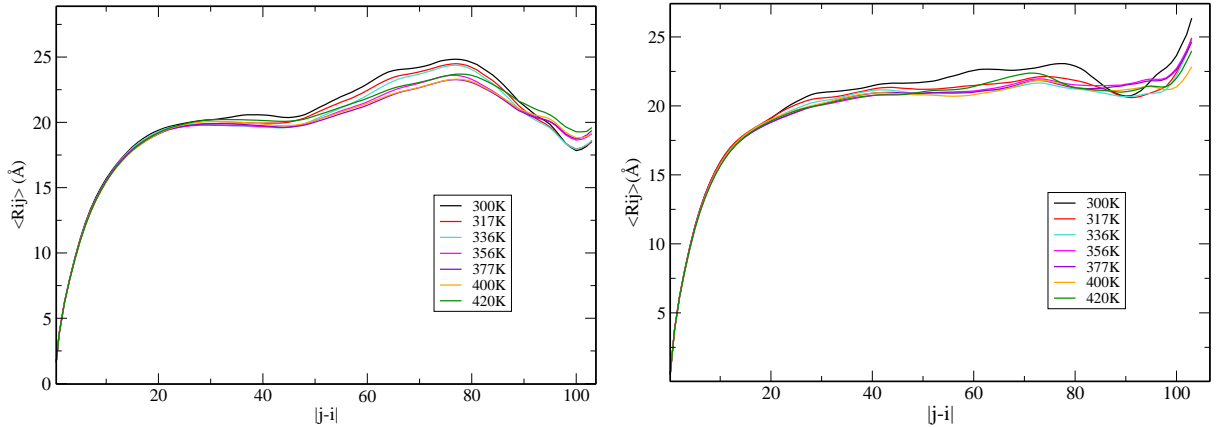


Figure 15: Temperature dependence of $\langle R_{ij} \rangle$ profiles for V form (left) and M form (right). No evident relationship can be seen with increasing temperature in the packing of the globule.

4 Research Design

Aim1: Characterizing the conformational ensemble of wild type proBDNF

and Val66Met mutant. As discussed in the **Section 2: Background**, there is no experimentally-determined structure available for proBDNF. To investigate the effect of the mutation on the protein the first step is to construct the structure of proBDNF. Ten different prodomain conformations for both wild type and mutant proteins (generated in the preliminary studies) will be selected and attached to the N-terminus of the mBDNF crystal structure. Each generated structure then will be simulated using MD with enhanced sampling (**Section 5: General Procedures**). Then the resulting simulations will be analyzed to characterize the structure and dynamics of wild type and mutant proBDNF using the measures described in the **Section 3: Preliminary Studies**. The results will contribute to better understanding of the effect of mutation on isolated proBDNF.

As mentioned before experimental methods have indicated the interaction of prodomain with mature domain in proNGF which is a proBDNF homologue. Our simulations will also be analyzed to investigate the presence of prodomain interaction with mBDNF and if it is affected by the mutation.

As discussed in **Section 2: Background**, mBDNF binds to both p75^{NTR} and TrkB. Compared to mBDNF, proBDNF has higher affinity for p75^{NTR} and lower affinity for TrkB. We will therefore analyze our simulations to explore if the presence of prodomain changes the surface availability of residues on mBDNF or induces local conformational changes in mBDNF. In addition, the conformational ensemble of prodomain will be compared to the ensemble from isolated prodomain simulations to identify any changes due

to presence of mBDNF.

Aim 2: Characterizing the conformational ensemble of proBDNF in complex with its receptor p75^{NTR}. As discussed in **Section 2: Background**, proBDNF forms a high affinity ternary complex with Sortilin and p75^{NTR}. Experimental studies show that the homologue NGF prodomain interacts specifically with Sortilin and not p75^{NTR}, while mature domain interacts specifically with p75^{NTR} and not Sortilin. Also when proNGF is in complex with p75^{NTR} the prodomain shows higher affinity for Sortilin compared to isolated proNGF prodomain. To investigate the residues involved in interaction with p75^{NTR} and also the effect of p75^{NTR} on the dynamics and conformation of proBDNF we will first construct proBDNF:p75^{NTR} complex and then study the structure using MD simulations.

To construct the complex we will use the crystal structure of proNGF bound to p75^{NTR} as a template for homology modeling. The crystal structure doesn't have prodomain part which is expected due to its disordered nature. Therefore we will build the model using proBDNF structures generated in the previous aim. Multiple conformations will then be selected and studied using MD simulations with enhanced sampling (**Section 5: General Procedures**). The results will be analyzed to identify the residues that are directly involved in binding and also the presence of local conformational changes in proBDNF due to p75^{NTR}.

Aim 3: Characterizing the conformational ensemble of juxtamembrane domain of p75^{NTR}. As discussed in **Section 2: Background**, the juxtamembrane domain of p75^{NTR} is critical in propagation of conformational changes from extracellular

domain to the death domain upon ligand binding. Interestingly, while different neurotrophins bind to p75^{NTR} and induce different responses, the conformational changes are relayed through the same transmembrane and juxtamembrane domains. This could be due to other proteins being involved or the signal transducing domains adopt different conformations in response to each ligand.

There are some evidence indicating that transmembrane proteins can have disordered juxtamembrane domains[87] which can adopt many conformations and also bind different proteins. Homology modeling will be used to construct the transmembrane and juxtamembrane domains of p75^{NTR}. Then we will use MD simulations with enhanced sampling (**Section 5: General Procedures**) to explore the conformational ensembles that they can adopt. The presence of distinct but populated ensembles can indicate each ensemble might have different effect on the propagating signal from extracellular domain. The results will also contribute to better understanding of the conformations that disordered proteins can adopt in the presence of a membrane.

5 General Procedures

Homology Modelling MODELLER9.13[88] was used for comparative modeling of protein three dimensional structure. Several models will be generated and the one with the lowest MODELLER objective function will be used.

Molecular Dynamics Simulations Gromacs 4.6.3[89] molecular dynamics package with AMBER99SB-IDLN[82] force field will be used for the simulations.

Enhanced Sampling Methods The computational demanding nature of molecular simulations restricts the simulation time, thus, prevents a simulation from reaching biologically relevant time scales. To address the sampling problem several enhanced sampling techniques have been developed which allows to efficiently explore the configurational space in relatively shorter simulation time. Few of these methods are discussed below:

1) Temperature Replica Exchange(T-REMD) [90]: In REMD simulations, several replicas of a system are simulated independently and simultaneously at different temperatures. At specified intervals, replicas with neighboring temperatures are exchanged with the Boltzmann weighted metropolis criterion:

$$P_{swap}(i, j) = \min\{1, \exp((\beta_i - \beta_j)(U_i - U_j))\}$$

where $\beta = 1/k_B T$ and U is the potential energy. The random walk in temperatures allow systems trapped in metastable states to escape by exchanging replicas with system at higher temperatures.

T-REMD is easy to implement and is embarrassingly parallel but number of replicas required increases with system size and also large amount of time is spent in simulating at unrealistic temperatures[78]. Rendering T-REMD simulations of large proteins in an explicit solvent can be very demanding in computational terms.

2) Hamiltonian Replica Exchange(H-REMD) [91, 92]: It is a more generalized form of REMD. Since the Boltzmann factor only depends on $U/(k_B T)$, a double temperature is completely equivalent to a halved energy. Thus, scaling the Hamiltonian is

equivalent to scaling the temperature. The advantage of scaling the potential energy instead of the temperature is related to the fact that energy is an extensive property and unlike temperature one can selectively choose a portion of the system (only the prodomain in our case) to be 'Heated'.

Heating only a part of the system also reduces the number of replicas in a given temperature range, thus improving the computational efficiency. However, for implementing H-REMD force-field parameters have to be rescaled also, they are not always very efficient in protein folding simulations[93]

3) Accelerated Molecular Dynamics(aMD) [94]: In aMD, increased conformational sampling is obtained by applying a biasing potential (boost potential) to part or all of the system when the potential energy drops below a user-specified energy cutoff,

$E_{\text{threshold}}$.

$$V^*(r) = \begin{cases} V(r) & V(r) \geq E_{\text{threshold}} \\ V(r) + E_{\text{boost}}(r) & V(r) < E_{\text{threshold}} \end{cases}$$

Here \mathbf{r} represents the coordinates of the system, $V^*(r)$ is the boosted potential, $V(r)$ is the unmodified potential, and $E_{\text{boost}}(r)$ is the boost potential. The original form of the boost potential is

$$E_{\text{boost}}(r) = \frac{(E_{\text{threshold}} - V(r))^2}{\alpha + (E_{\text{threshold}} - V(r))}$$

The resulting conformational ensemble is biased, and in practice, reweighing biased ensembles such as those obtained from aMD simulations can be challenging. Also, the

values of Ethreshold and α have to be chosen appropriately[95].

Various combinations of above defined methods is also possible and have been implemented efficiently[95, 96, 78, 97]

References

- [1] Celeste J Brown, Audra K Johnson, A Keith Dunker, and Gary W Daughdrill. Evolution and disorder. *Current opinion in structural biology*, 21(3):441–6, June 2011.
- [2] Jinfeng Liu, Yan Zhang, Xingye Lei, and Zemin Zhang. Natural selection of protein structural and functional properties: a single nucleotide polymorphism perspective. *Genome biology*, 9(4):R69, January 2008.
- [3] Vladimir Vacic, Phineus R L Markwick, Christopher J Oldfield, Xiaoyue Zhao, Chad Haynes, Vladimir N Uversky, and Lilia M Iakoucheva. Disease-associated mutations disrupt functionally important regions of intrinsic protein disorder. *PLoS computational biology*, 8(10):e1002709, January 2012.
- [4] Oliver C Redfern, Benoit Dessailly, and Christine a Orengo. Exploring the structure and function paradigm. *Current opinion in structural biology*, 18(3):394–402, June 2008.
- [5] Wei-Lun Hsu, Christopher Oldfield, Jingwei Meng, Fei Huang, Bin Xue, Vladimir N Uversky, Pedro Romero, and a Keith Dunker. Intrinsic protein disorder and protein-protein interactions. *Pacific Symposium on Biocomputing. Pacific Symposium on Biocomputing*, pages 116–27, January 2012.

- [6] Jiawen Wu, Dungeng Peng, Markus Voehler, Charles R Sanders, and Jun Li. Structure and expression of a novel compact myelin protein - small VCP-interacting protein (SVIP). *Biochemical and biophysical research communications*, 440(1):173–8, October 2013.
- [7] H Jane Dyson, Peter E Wright, and North Torrey Pines. Intrinsically unstructured proteins and their functions. *Nat Rev Mol Cell Biol*, 6(3), March 2005.
- [8] Albert H Mao, Scott L Crick, Andreas Vitalis, Caitlin L Chicoine, and Rohit V Pappu. Net charge per residue modulates conformational ensembles of intrinsically disordered proteins. *Proceedings of the National Academy of Sciences of the United States of America*, 107(18):8183–8, May 2010.
- [9] Rahul K. Das and Rohit V. Pappu. Conformations of intrinsically disordered proteins are influenced by linear sequence distributions of oppositely charged residues. *Proceedings of the National Academy of Sciences*, 110(33):13392–13397, 2013.
- [10] Megan Sickmeier, Justin A. Hamilton, Tanguy LeGall, Vladimir Vacic, Marc S. Cortese, Agnes Tantos, Beata Szabo, Peter Tompa, Jake Chen, Vladimir N. Uversky, Zoran Obradovic, and A. Keith Dunker. Disprot: the database of disordered proteins. *Nucleic Acids Research*, 35(suppl 1):D786–D793, 2007.
- [11] V N Uversky, J R Gillespie, and a L Fink. Why are "natively unfolded" proteins unstructured under physiologic conditions? *Proteins*, 41(3):415–27, November 2000.
- [12] P Romero, Z Obradovic, X Li, E C Garner, C J Brown, and a K Dunker. Sequence complexity of disordered protein. *Proteins*, 42(1):38–48, January 2001.

- [13] Zsuzsanna Dosztányi, Veronika Csizmók, Péter Tompa, and István Simon. The pairwise energy content estimated from amino acid composition discriminates between folded and intrinsically unstructured proteins. *Journal of molecular biology*, 347(4):827–39, April 2005.
- [14] R M Williams, Z Obradovi, V Mathura, W Braun, E C Garner, J Young, S Takayama, C J Brown, and A K Dunker. The protein non-folding problem: amino acid determinants of intrinsic order and disorder. *Pacific Symposium on Biocomputing. Pacific Symposium on Biocomputing*, pages 89–100, January 2001.
- [15] Bo He, Kejun Wang, Yunlong Liu, Bin Xue, Vladimir N Uversky, and a Keith Dunker. Predicting intrinsic disorder in proteins: an overview. *Cell research*, 19(8):929–49, August 2009.
- [16] J J Ward, J S Sodhi, L J McGuffin, B F Buxton, and D T Jones. Prediction and functional analysis of native disorder in proteins from the three kingdoms of life. *Journal of molecular biology*, 337(3):635–45, March 2004.
- [17] Vladimir N Uversky. A decade and a half of protein intrinsic disorder: biology still waits for physics. *Protein science : a publication of the Protein Society*, 22(6):693–724, June 2013.
- [18] Monika Fuxreiter, Peter Tompa, István Simon, Vladimir N Uversky, Jeffrey C Hansen, and Francisco J Asturias. regulation. *Nat Chem Biol*, 4(12):728–737, 2010.
- [19] Christopher J Oldfield, Jingwei Meng, Jack Y Yang, Mary Qu Yang, Vladimir N Uversky, and a Keith Dunker. Flexible nets: disorder and induced fit in the associa-

tions of p53 and 14-3-3 with their partners. *BMC genomics*, 9(Suppl 1):S1, January 2008.

- [20] B a Shoemaker, J J Portman, and P G Wolynes. Speeding molecular recognition by using the folding funnel: the fly-casting mechanism. *Proceedings of the National Academy of Sciences of the United States of America*, 97(16):8868–73, August 2000.
- [21] Madoka Akimoto, Rajeevan Selvaratnam, E Tyler McNicholl, Geeta Verma, Susan S Taylor, and Giuseppe Melacini. Signaling through dynamic linkers as revealed by PKA. *Proceedings of the National Academy of Sciences of the United States of America*, 110(35):14231–6, August 2013.
- [22] P.E. Wright and H.J. Dyson. Linking folding and binding. *Current Opinion in Structural Biology*, 19(1):31–38, 2009.
- [23] Iskra Staneva, Yongqi Huang, Zhirong Liu, and Stefan Wallin. Binding of two intrinsically disordered peptides to a multi-specific protein: a combined Monte Carlo and molecular dynamics study. *PLoS computational biology*, 8(9):e1002682, January 2012.
- [24] Peter Tompa and Monika Fuxreiter. Fuzzy complexes: polymorphism and structural disorder in proteinprotein interactions. *Trends in Biochemical Sciences*, 33(1):2–8, 2008.
- [25] Fan Jin, Chen Yu, Luhua Lai, and Zhirong Liu. Ligand clouds around protein clouds: a scenario of ligand binding with intrinsically disordered proteins. *PLoS computational biology*, 9(10):e1003249, January 2013.

- [26] James M. Krieger, Giuliana Fusco, Marc Lewitzky, Philip C. Simister, Jan Marchant, Carlo Camilloni, Stephan M. Feller, and Alfonso De Simone. Conformational Recognition of an Intrinsically Disordered Protein. *Biophysical Journal*, 106(8):1771–1779, April 2014.
- [27] P Ojeda-May and Jingzhi Pu. Replica exchange molecular dynamics simulations of an α/β -type small acid soluble protein (SASP). *Biophysical chemistry*, 184:17–21, December 2013.
- [28] Luca Larini, Megan Murray Gessel, Nichole E LaPointe, Thanh D Do, Michael T Bowers, Stuart C Feinstein, and Joan-Emma Shea. Initiation of assembly of tau(273–284) and its Δ K280 mutant: an experimental and computational study. *Physical chemistry chemical physics : PCCP*, 15(23):8916–28, June 2013.
- [29] Ewa A Bienkiewicz, Joshua N Adkins, and Kevin J Lumb. Functional consequences of preorganized helical structure in the intrinsically disordered cell-cycle inhibitor p27(Kip1). *Biochemistry*, 41(3):752–9, January 2002.
- [30] Timothy H Click, Debabani Ganguly, and Jianhan Chen. Intrinsically disordered proteins in a physics-based world. *International journal of molecular sciences*, 11(12):5292–309, January 2010.
- [31] Michael Knott and Robert B Best. A preformed binding interface in the unbound ensemble of an intrinsically disordered protein: evidence from molecular simulations. *PLoS computational biology*, 8(7):e1002605, January 2012.
- [32] Hyungju Park and Mu-ming Poo. Neurotrophin regulation of neural circuit development and function. *Nature reviews. Neuroscience*, 14(1):7–23, January 2013.

- [33] Kenneth K. Teng, Sarah Felice, Taeho Kim, and Barbara L. Hempstead. Understanding proneurotrophin actions: Recent advances and challenges. *Developmental Neurobiology*, 70(5):350–359, 2010.
- [34] S Cohen, R Levi-Montalcini, and V Hamburger. A NERVE GROWTH-STIMULATING FACTOR ISOLATED FROM SARCOM AS 37 AND 180. *Proc Natl Acad Sci U S A*, 40(10):1014–8, October 1954.
- [35] R Levi-Montalcini. The nerve growth factor: thirty-five years later. *The EMBO journal*, 6(5):1145–54, May 1987.
- [36] Y A Barde, D Edgar, and H Thoenen. Purification of a new neurotrophic factor from mammalian brain. *The EMBO journal*, 1(5):549–53, January 1982.
- [37] P. Maisonpierre, L Belluscio, S Squinto, N. Ip, M. Furth, R. Lindsay, and G. Yan-copoulos. Neurotrophin-3: a neurotrophic factor related to NGF and BDNF. *Science*, 247(4949):1446–1451, March 1990.
- [38] N. Y. Ip, C. F. Ibanez, S. H. Nye, J. McClain, P. F. Jones, D. R. Gies, L. Bel-luscio, M. M. Le Beau, R. Espinosa, and S. P. Squinto. Mammalian neurotrophin-4: structure, chromosomal localization, tissue distribution, and receptor specificity. *Proceedings of the National Academy of Sciences*, 89(7):3060–3064, April 1992.
- [39] U Suter, J V Heymach, and E M Shooter. Two conserved domains in the NGF propeptide are necessary and sufficient for the biosynthesis of correctly processed and biologically active NGF. *The EMBO journal*, 10(9):2395–400, September 1991.

- [40] John V. Heymach and Eric M. Shooter. The biosynthesis of neurotrophin heterodimers by transfected mammalian cells. *Journal of Biological Chemistry*, 270(20):12297–12304, 1995.
- [41] Roland Kolbeck, Stefan Jungbluth, and Yves-Alain Barde. Characterisation of neurotrophin dimers and monomers. *European Journal of Biochemistry*, 225(3):995–1003, 1994.
- [42] Yves-Alain Barde. The nerve growth factor family. *Progress in Growth Factor Research*, 2(4):237 – 248, 1990.
- [43] Francesca Paoletti, Francesca Malerba, Geoff Kelly, Sylvie Noinville, Doriano Lamba, Antonino Cattaneo, and Annalisa Pastore. Conformational plasticity of proNGF. *PloS one*, 6(7):e22615, January 2011.
- [44] Agustin Anastasia, Katrin Deinhardt, Moses V Chao, Nathan E Will, Krithi Irmady, Francis S Lee, Barbara L Hempstead, and Clay Bracken. Val66Met polymorphism of BDNF alters prodomain structure to induce neuronal growth cone retraction. *Nature communications*, 4:2490, January 2013.
- [45] M. Korte, P. Carroll, E. Wolf, G. Brem, H. Thoenen, and T. Bonhoeffer. Hippocampal long-term potentiation is impaired in mice lacking brain-derived neurotrophic factor. *Proceedings of the National Academy of Sciences*, 92(19):8856–8860, September 1995.
- [46] Zhe-Yu Chen, Kevin Bath, Bruce McEwen, Barbara Hempstead, and Francis Lee. Impact of genetic variant BDNF (Val66Met) on brain structure and function. *Novartis Foundation symposium*, 289:180–8, January 2008.

- [47] Seidah N, Benjannet S, Pareek S, Savaria D, Hamelin J, Goulet B, Laliberte J, Lazure C, Chretien M, and Murphy R. Cellular processing of the nerve growth factor precursor by the mammalian pro-protein convertases. *Biochem J.*, 314:951960, March 1996.
- [48] Petti T Pang and Bai Lu. Regulation of late-phase LTP and long-term memory in normal and aging hippocampus: role of secreted proteins tPA and BDNF. *Ageing research reviews*, 3(4):407–30, November 2004.
- [49] Philip a Barker. Whither proBDNF? *Nature neuroscience*, 12(2):105–6, February 2009.
- [50] Manish J. Butte, Peter K. Hwang, William C. Mobley, and Robert J. Fletterick. Crystal structure of neurotrophin-3 homodimer shows distinct regions are used to bind its receptors,. *Biochemistry*, 37(48):16846–16852, 1998.
- [51] N Q McDonald, R Lapatto, J Murray-Rust, J Gunning, A Wlodawer, and T L Blundell. New protein fold revealed by a 2.3-A resolution crystal structure of nerve growth factor. *Nature*, 354(6352):411–4, December 1991.
- [52] R C Robinson, C Radziejewski, G Spraggan, J Greenwald, M R Kostura, L D Burtnick, D I Stuart, S Choe, and E Y Jones. The structures of the neurotrophin 4 homodimer and the brain-derived neurotrophic factor/neurotrophin 4 heterodimer reveal a common Trk-binding site. *Protein science : a publication of the Protein Society*, 8(12):2589–97, December 1999.

- [53] C Wiesmann, M H Ultsch, S H Bass, and a M de Vos. Crystal structure of nerve growth factor in complex with the ligand-binding domain of the TrkA receptor. *Nature*, 401(6749):184–8, September 1999.
- [54] M J Banfield, R L Naylor, A G Robertson, S J Allen, D Dawbarn, and R L Brady. Specificity in Trk receptor:neurotrophin interactions: the crystal structure of TrkB-d5 in complex with neurotrophin-4/5. *Structure (London, England : 1993)*, 9(12):1191–9, December 2001.
- [55] Marco Kliemann, Ralph Golbik, Rainer Rudolph, Elisabeth Schwarz, and Hauke Lilie. The pro-peptide of prongf: Structure formation and intramolecular association with ngf. *Protein Science*, 16(3):411–419, 2007.
- [56] Dan Feng, Taeho Kim, Engin Ozkan, Matthew Light, Risa Torkin, Kenneth K Teng, Barbara L Hempstead, and K Christopher Garcia. Molecular and structural insight into proNGF engagement of p75NTR and sortilin. *Journal of molecular biology*, 396(4):967–84, March 2010.
- [57] Zhe-Yu Chen, Alessandro Ieraci, Henry Teng, Henning Dall, Chui-Xiang Meng, Daniel G Herrera, Anders Nykjaer, Barbara L Hempstead, and Francis S Lee. Sortilin controls intracellular sorting of brain-derived neurotrophic factor to the regulated secretory pathway. *The Journal of neuroscience : the official journal of the Society for Neuroscience*, 25(26):6156–66, June 2005.
- [58] Anders Nykjaer, Ramee Lee, Kenneth K Teng, and Pernille Jansen. Sortilin is essential for proNGF- induced neuronal cell death. *Nature*, 427(6977):15–20, 2004.

- [59] Jacqueline Boutilier, Claire Ceni, Promila C Pagdala, Alison Forgie, Kenneth E Neet, and Philip A Barker. Proneurotrophins require endocytosis and intracellular proteolysis to induce TrkA activation. *The Journal of biological chemistry*, 283(19):12709–16, May 2008.
- [60] R Lee, P Kermani, K K Teng, and B L Hempstead. Regulation of cell survival by secreted proneurotrophins. *Science*, 294(5548):1945–8, November 2001.
- [61] Newton H Woo, Henry K Teng, Chia-Jen Siao, Cristina Chiaruttini, Petti T Pang, Teresa a Milner, Barbara L Hempstead, and Bai Lu. Activation of p75NTR by proBDNF facilitates hippocampal long-term depression. *Nature neuroscience*, 8(8):1069–77, August 2005.
- [62] Henry K Teng, Kenneth K Teng, Ramee Lee, Saundrene Wright, Seema Tevar, Ramiro D Almeida, Pouneh Kermani, Risa Torkin, Zhe-Yu Chen, Francis S Lee, Rosemary T Kraemer, Anders Nykjaer, and Barbara L Hempstead. ProBDNF induces neuronal apoptosis via activation of a receptor complex of p75NTR and sortilin. *The Journal of neuroscience : the official journal of the Society for Neuroscience*, 25(22):5455–63, June 2005.
- [63] Ying Sun, Yoon Lim, Fang Li, Shen Liu, Jian-Jun Lu, Rainer Haberberger, Jin-Hua Zhong, and Xin-Fu Zhou. ProBDNF collapses neurite outgrowth of primary neurons by activating RhoA. *PloS one*, 7(4):e35883, January 2012.
- [64] Katrin Deinhardt, Taeho Kim, Daniel S Spellman, Richard E Mains, Betty a Eipper, Thomas a Neubert, Moses V Chao, and Barbara L Hempstead. Neuronal growth

cone retraction relies on proneurotrophin receptor signaling through Rac. *Science signaling*, 4(202):ra82, January 2011.

- [65] D Johnson, A Lanahan, C R Buck, A Sehgal, C Morgan, E Mercer, M Bothwell, and M Chao. Expression and structure of the human NGF receptor. *Cell*, 47(4):545–54, November 1986.
- [66] Georg Dechant and Yves-Alain Barde. The neurotrophin receptor p75(NTR): novel functions and implications for diseases of the nervous system. *Nature neuroscience*, 5(11):1131–6, November 2002.
- [67] Maral Vilar, Ioannis Charalampopoulos, Rajappa S. Kenchappa, Anastasia Simi, Esra Karaca, Alessandra Reversi, Soyoung Choi, Mark Bothwell, Ismael Mingarro, Wilma J. Friedman, Giampietro Schiavo, Philippe I.H. Bastiaens, Peter J. Verveer, Bruce D. Carter, and Carlos F. Ibez. Activation of the p75 neurotrophin receptor through conformational rearrangement of disulphide-linked receptor dimers. *Neuron*, 62(1):72 – 83, 2009.
- [68] Yong Gong, Peng Cao, Hong-jun Yu, and Tao Jiang. Crystal structure of the neurotrophin-3 and p75NTR symmetrical complex. *Nature*, 454(7205):789–93, August 2008.
- [69] E Liepinsh, L L Ilag, G Otting, and C F Ibáñez. NMR structure of the death domain of the p75 neurotrophin receptor. *The EMBO journal*, 16(16):4999–5005, August 1997.
- [70] Sandra Dieni, Tomoya Matsumoto, Martijn Dekkers, Stefanie Rauskolb, Mihai S Ionescu, Ruben Deogracias, Eckart D Gundelfinger, Masami Kojima, Sigrun Nestel,

Michael Frotscher, and Yves-Alain Barde. BDNF and its pro-peptide are stored in presynaptic dense core vesicles in brain neurons. *The Journal of cell biology*, 196(6):775–88, March 2012.

- [71] Mònica Gratacòs, Juan R González, Josep M Mercader, Rafael de Cid, Mikel Urretavizcaya, and Xavier Estivill. Brain-derived neurotrophic factor Val66Met and psychiatric disorders: meta-analysis of case-control studies confirm association to substance-related disorders, eating disorders, and schizophrenia. *Biological psychiatry*, 61(7):911–22, April 2007.
- [72] Fatima Soliman, Charles E Glatt, Kevin G Bath, Liat Levita, Rebecca M Jones, Siobhan S Pattwell, Deqiang Jing, Nim Tottenham, Dima Amso, Leah H Somerville, Henning U Voss, Gary Glover, Douglas J Ballon, Conor Liston, Theresa Teslovich, Tracey Van Kempen, Francis S Lee, and B J Casey. A genetic variant BDNF polymorphism alters extinction learning in both mouse and human. *Science*, 327(5967):863–6, February 2010.
- [73] M Verhagen, A van der Meij, P A M van Deurzen, J G E Janzing, A Arias-Vásquez, J K Buitelaar, and B Franke. Meta-analysis of the BDNF Val66Met polymorphism in major depressive disorder: effects of gender and ethnicity. *Molecular psychiatry*, 15(3):260–71, March 2010.
- [74] Shiou-Lan Chen, Sheng-Yu Lee, Yun-Hsuan Chang, Shih-Heng Chen, Chun-Hsien Chu, Tzu-Yun Wang, Po-See Chen, I-Hui Lee, Yen-Kuang Yang, Jau-Shyong Hong, and Ru-Band Lu. The BDNF Val66Met polymorphism and plasma brain-derived neurotrophic factor levels in Han Chinese patients with bipolar disorder

- and schizophrenia. *Progress in neuro-psychopharmacology & biological psychiatry*, 51:99–104, June 2014.
- [75] Kevin G Bath, Deqiang Q Jing, Iva Dincheva, Christine C Neeb, Siobhan S Pat-twell, Moses V Chao, Francis S Lee, and Ipe Ninan. BDNF Val66Met impairs fluoxetine-induced enhancement of adult hippocampus plasticity. *Neuropsychopharmacology : official publication of the American College of Neuropsychopharmacology*, 37(5):1297–304, April 2012.
- [76] C Chiaruttini, A Vicario, Z Li, G Baj, P Braiuca, Y Wu, F S Lee, L Gardossi, J M Baraban, and E Tongiorgi. Dendritic trafficking of BDNF mRNA is mediated by translin and blocked by the G196A (Val66Met) mutation. *Proceedings of the National Academy of Sciences of the United States of America*, 106(38):16481–6, September 2009.
- [77] Michael F Egan, Masami Kojima, Joseph H Callicott, Terry E Goldberg, Bhaskar S Kolachana, Alessandro Bertolino, Eugene Zaitsev, Bert Gold, David Goldman, Michael Dean, Bai Lu, and Daniel R Weinberger. The BDNF val66met polymor-phism affects activity-dependent secretion of BDNF and human memory and hip-pocampal function. *Cell*, 112(2):257–69, January 2003.
- [78] Cameron Abrams and Giovanni Bussi. Enhanced sampling in molecular dynam-ics using metadynamics, replica-exchange, and temperature-acceleration. *Entropy*, 16(1):163–199, 2013.

- [79] Matthew C Zwier and Lillian T Chong. Reaching biological timescales with all-atom molecular dynamics simulations. *Current opinion in pharmacology*, 10(6):745–52, December 2010.
- [80] Jing Huang and Alexander D MacKerell. CHARMM36 all-atom additive protein force field: validation based on comparison to NMR data. *Journal of computational chemistry*, 34(25):2135–45, September 2013.
- [81] Viktor Hornak, Robert Abel, Asim Okur, Bentley Strockbine, Adrian Roitberg, and Carlos Simmerling. Comparison of multiple Amber force fields and development of improved protein backbone parameters. *Proteins*, 65(3):712–25, November 2006.
- [82] Kresten Lindorff-Larsen, Stefano Piana, Kim Palmo, Paul Maragakis, John L Klepeis, Ron O Dror, and David E Shaw. Improved side-chain torsion potentials for the Amber ff99SB protein force field. *Proteins*, 78(8):1950–8, June 2010.
- [83] Jaime Prilusky, Clifford E Felder, Tzviya Zeev-Ben-Mordehai, Edwin H Rydberg, Orna Man, Jacques S Beckmann, Israel Silman, and Joel L Sussman. FoldIndex: a simple tool to predict whether a given protein sequence is intrinsically unfolded. *Bioinformatics*, 21(16):3435–8, August 2005.
- [84] R. Linding. GlobPlot: exploring protein sequences for globularity and disorder. *Nucleic Acids Research*, 31(13):3701–3708, July 2003.
- [85] Jack Kyte and Russell F. Doolittle. A simple method for displaying the hydropathic character of a protein. *Journal of Molecular Biology*, 157(1):105 – 132, 1982.

- [86] Magnus Kjaergaard and Flemming M Poulsen. Sequence correction of random coil chemical shifts: correlation between neighbor correction factors and changes in the Ramachandran distribution. *Journal of biomolecular NMR*, 50(2):157–65, June 2011.
- [87] Ilias Stavropoulos, Nora Khaldi, Norman E Davey, Kevin O’Brien, Finian Martin, and Denis C Shields. Protein disorder and short conserved motifs in disordered regions are enriched near the cytoplasmic side of single-pass transmembrane proteins. *PloS one*, 7(9):e44389, January 2012.
- [88] Andrej ali and Tom L. Blundell. Comparative protein modelling by satisfaction of spatial restraints. *Journal of Molecular Biology*, 234(3):779 – 815, 1993.
- [89] Sander Pronk, Szilárd Páll, Roland Schulz, Per Larsson, Pär Bjelkmar, Rossen Apostolov, Michael R Shirts, Jeremy C Smith, Peter M Kasson, David van der Spoel, Berk Hess, and Erik Lindahl. GROMACS 4.5: a high-throughput and highly parallel open source molecular simulation toolkit. *Bioinformatics*, 29(7):845–54, April 2013.
- [90] Yuji Sugita and Yuko Okamoto. Replica-exchange molecular dynamics method for protein folding. *Chemical Physics Letters*, 314(1-2):141–151, November 1999.
- [91] Yuji Sugita, Akio Kitao, and Yuko Okamoto. Multidimensional replica-exchange method for free-energy calculations. *J. Chem. Phys.*, 113(15), 2000.
- [92] Hiroaki Fukunishi, Osamu Watanabe, and Shoji Takada. On the Hamiltonian replica exchange method for efficient sampling of biomolecular systems: Application to protein structure prediction. *The Journal of Chemical Physics*, 116(20):9058, May 2002.

- [93] Tsuyoshi Terakawa, Tomoshi Kameda, and Shoji Takada. On easy implementation of a variant of the replica exchange with solute tempering in gromacs. *Journal of Computational Chemistry*, 32(7):1228–1234, 2011.
- [94] Donald Hamelberg, John Mongan, and J Andrew McCammon. Accelerated molecular dynamics: a promising and efficient simulation method for biomolecules. *The Journal of chemical physics*, 120(24):11919–29, June 2004.
- [95] Daniel R Roe, Christina Bergonzo, and Thomas E Cheatham. Evaluation of enhanced sampling provided by accelerated molecular dynamics with hamiltonian replica exchange methods. *The journal of physical chemistry. B*, 118(13):3543–52, April 2014.
- [96] Asim Okur, Lauren Wickstrom, Melinda Layten, Raphäel Geney, Kun Song, Viktor Hornak, and Carlos Simmerling. Improved Efficiency of Replica Exchange Simulations through Use of a Hybrid Explicit/Implicit Solvation Model. *Journal of Chemical Theory and Computation*, 2(2):420–433, March 2006.
- [97] Katja Ostermeir and Martin Zacharias. Advanced replica-exchange sampling to study the flexibility and plasticity of peptides and proteins. *Biochimica et biophysica acta*, 1834(5):847–53, May 2013.